

The Open University's repository of research publications
and other research outputs

Early fluid activity on Ryugu inferred by isotopic analyses of carbonates and magnetite

Journal Item

How to cite:

McCain, Kaitlyn A.; Matsuda, Nozomi; Liu, Ming-Chang; McKeegan, Kevin D.; Yamaguchi, Akira; Kimura, Makoto; Tomioka, Naotaka; Ito, Motoo; Imae, Naoya; Uesugi, Masayuki; Shirai, Naoki; Ohigashi, Takuji; Greenwood, Richard C.; Uesugi, Kentaro; Nakato, Aiko; Yogata, Kasumi; Yuzawa, Hayato; Kodama, Yu; Hirahara, Kaori; Sakurai, Ikuya; Okada, Ikuo; Karouji, Yuzuru; Nakazawa, Satoru; Okada, Tatsuaki; Saiki, Takanao; Tanaka, Satoshi; Terui, Fuyuto; Yoshikawa, Makoto; Miyazaki, Akiko; Nishimura, Masahiro; Yada, Toru; Abe, Masanao; Usui, Tomohiro; Watanabe, Sei-ichiro and Tsuda, Yuichi (2023). Early fluid activity on Ryugu inferred by isotopic analyses of carbonates and magnetite. *Nature Astronomy* (Early Access).

For guidance on citations see [FAQs](#).

© 2023 The Authors



<https://creativecommons.org/licenses/by/4.0/>

Version: Submitted Version

Link(s) to article on publisher's website:

<http://dx.doi.org/doi:10.1038/s41550-022-01863-0>

Copyright and Moral Rights for the articles on this site are retained by the individual authors and/or other copyright owners. For more information on Open Research Online's data [policy](#) on reuse of materials please consult the policies page.

Early fluid activity on Ryugu: perspectives from oxygen, carbon, and ^{53}Mn - ^{53}Cr isotopes

Kaitlyn McCain

UCLA

Nozomi Matsuda (✉ nozomi32@ucla.edu)

University of California, Los Angeles <https://orcid.org/0000-0003-3461-0547>

Ming-Chang Liu

Department of Earth, Planetary, and Space Sciences, UCLA <https://orcid.org/0000-0003-4030-5258>

Kevin McKeegan

UCLA

Akira Yamaguchi

National Institute of Polar Research

Makoto Kimura

National Institute of Polar Research

Naotaka Tomioka

Japan Agency for Marine-Earth Science and Technology <https://orcid.org/0000-0001-5725-9513>

Motoo Ito

Japan Agency for Marine-Earth Science and Technology <https://orcid.org/0000-0001-5686-0243>

Naoya Imae

National Institute of Polar Research

Masayuki Uesugi

JASRI/SPring-8 <https://orcid.org/0000-0001-6261-9034>

Naoki Shirai

Kanagawa University

Takuji Ohigashi

High Energy Accelerator Research Organization <https://orcid.org/0000-0003-4778-5645>

Richard Greenwood

The Open University

Kentaro Uesugi

Japan Synchrotron Radiation Research Institute <https://orcid.org/0000-0003-2579-513X>

Aiko Nakato

Japan Aerospace Exploration Agency <https://orcid.org/0000-0003-2392-1497>

Kasumi Yogata

JAXA

Hayato Yuzawa

UVSOR/IMS <https://orcid.org/0000-0003-4129-4407>

Yu Kodama

Marine Works Japan, Ltd

Kaori Hirahara

Osaka University <https://orcid.org/0000-0002-7776-4493>

Ikuya Sakurai

Nagoya University

Ikuo Okada

Nagoya University

Yuzuru Karouji

Japan Aerospace Exploration Agency <https://orcid.org/0000-0002-8540-2986>

Satoru Nakazawa

Japan Aerospace Exploration Agency <https://orcid.org/0000-0003-4250-1826>

Tatsuaki Okada

Japan Aerospace Exploration Agency <https://orcid.org/0000-0001-6381-8107>

Takanao Saiki

Japan Aerospace Exploration Agency

Satoshi Tanaka

JAXA

Fuyuto Terui

Kanagawa Institute of Technology

Makoto Yoshikawa

Japan Aerospace Exploration Agency

Akiko Miyazaki

JAXA <https://orcid.org/0000-0001-7427-2285>

Masahiro Nishimura

JAXA

Toru Yada

Japan Aerospace Exploration Agency <https://orcid.org/0000-0002-7971-510X>

Masanao Abe

Japan Aerospace Exploration Agency

Tomohiro Usui

JAXA <https://orcid.org/0000-0002-4653-293X>

Sei-ichiro Watanabe

Nagoya University <https://orcid.org/0000-0002-5820-2102>

Yuichi Tsuda

Japan Aerospace Exploration Agency

Article

Keywords:

Posted Date: June 8th, 2022

DOI: <https://doi.org/10.21203/rs.3.rs-1647235/v1>

License:   This work is licensed under a Creative Commons Attribution 4.0 International License.

[Read Full License](#)

Version of Record: A version of this preprint was published at Nature Astronomy on January 12th, 2023. See the published version at <https://doi.org/10.1038/s41550-022-01863-0>.

Abstract

Samples from asteroid Ryugu returned by the Hayabusa2 mission contain evidence of extensive alteration by aqueous fluids and appear related to the CI chondrites. To understand the sources of the fluid and the timing of chemical reactions occurring during the alteration processes, we investigated the oxygen, carbon, and ^{53}Mn - ^{53}Cr systematics of carbonate and magnetite in two Ryugu particles. We find that the fluid was initially between 0 – 20°C and enriched in ^{13}C , and ^{17}O and ^{18}O , and subsequently evolved towards lighter carbon and oxygen isotopic compositions as alteration proceeded. Carbonate ages show that this fluid-rock interaction took place within the first ~ 1.4 million years of solar system history requiring early accretion and preservation of carbonaceous material, either in a planetesimal less than ~ 17 km in diameter or a larger body which was disrupted and reassembled.

Introduction

The Hayabusa2 mission returned approximately 5.4 g of material from the C-type asteroid Ryugu. This material is highly aqueously altered and resembles the rare CI (Ivuna-type) chondrite meteorites, with abundant Mg-phyllsilicate, pyrrhotite, magnetite, and carbonate recording extensive fluid evolution on Ryugu's parent body¹⁻³. Because aqueous alteration products such as magnetite and carbonate record information about the fluid from which they form, isotopic measurements of these components can be used to constrain the timing and characteristics of aqueous alteration of Ryugu materials.

In addition to their mineralogical similarities, the bulk oxygen isotopic compositions of the Ryugu particles and CI chondrites are also similar in $\Delta^{17}\text{O}^4$. These values are primarily defined by the phyllosilicate matrix, the most abundant component in both Ryugu and the CI chondrites. Oxygen isotopic compositions of CI components such as carbonate, anhydrous silicate, phyllosilicate, and magnetite have been used to estimate the temperatures of final equilibration between carbonate and phyllosilicate to ~ 50–150°C^{5,6}, and radiometric dating of secondary minerals has constrained the timing of fluid alteration to ~ 4–6 Myr after CAI formation^{7,8}. However, the CI chondrites have been exposed to various degrees of terrestrial alteration, which appear to have affected the bulk oxygen isotopic compositions⁴. Ryugu particles therefore represent a unique opportunity to study pristine samples of hydrated asteroidal material.

Of the various alteration products found in hydrated extraterrestrial materials like returned Ryugu particles and CI chondrites, carbonate minerals are of particular interest because they can be dated using the short-lived ^{53}Mn - ^{53}Cr chronometer ($t_{1/2} = 3.7$ Myr), thereby tracking when liquid water was present and establishing a timescale for the accretion and alteration of carbonaceous planetesimals. Stable isotope studies of the major elements O and C can also provide insight into the sources of the fluids present as well as the temperatures and reactions occurring in the asteroid or its progenitor. To preserve the petrologic context and minimize consumption of precious Ryugu material, these analyses can be performed in-situ with high spatial resolution using Secondary Ion Mass Spectrometry (SIMS) to sputter

material from individual mineral grains with a spot size of $\sim 3\text{--}15\ \mu\text{m}$ (see Supplementary Methods). This technique has also been applied to analyses of carbonate and other secondary minerals in CM and CI carbonaceous chondrites, which facilitates comparison between the returned Ryugu particles and previously-studied meteorite samples.

The oxygen isotopic systematics of aqueous alteration products in carbonaceous chondrite meteorites have been extensively studied^{6,9-20} and used to infer the extent of equilibration between co-accreted water ice, inferred to be $^{17,18}\text{O}$ -enriched²¹ with positive $\Delta^{17}\text{O}$, and primary, anhydrous silicates^{5,20,22} with negative $\Delta^{17}\text{O}$ on the parent body, thereby tracking the sequence of alteration. In addition, if two secondary phases with the same $\Delta^{17}\text{O}$ are identified, the difference in $\delta^{18}\text{O}$ between the two phases can be used to calculate an equilibrium formation temperature, based on the assumption that they precipitated from the same water composition^{5,9,10,19}. For the CI chondrites, temperatures of aqueous alteration have been estimated to be $\sim 50\text{--}150^\circ\text{C}$ based upon the phyllosilicate-carbonate pair^{5,6}. The oxygen isotopic compositions of magnetite, if found to be in equilibrium with other secondary phases, can be used in a similar fashion¹⁹.

The carbon isotopic compositions of carbonate have been used to infer the contributions of various C sources, such as insoluble and soluble organic matter^{23,24} and isotopically heavy $\text{CO}_2\text{--CO}$ ices^{25,26}, to the fluids in the carbonaceous chondrite parent bodies. In addition, carbon isotope compositions can track reactions occurring within the fluid such as methane formation and loss^{15,18,19,27}, oxidation of organic material^{14,16}, and $\text{CH}_4\text{--CO}$ equilibration^{19,28}. However, such studies have thus far been limited to carbonate from CM (Mighei-type) chondrites; no in-situ C isotopic measurements have been conducted on CI carbonate.

The timing and duration of these chemical changes can be constrained using Mn-Cr dating, and these ages can also be used to constrain the accretion time of the parent bodies from which samples originate. Carbonate minerals are an ideal target for this analysis as they strongly fractionate Mn from Cr during their formation, leading to large excesses in ^{53}Cr through which a $^{53}\text{Mn}/^{55}\text{Mn}$ ratio at the time of carbonate formation can be inferred. Previous in-situ studies of highly-altered carbonaceous chondrites have found that most carbonate in these meteorite classes formed between 4–6 Myr after CAI formation in large ($> 50\ \text{km}$ radius) parent bodies which accreted 3–4 Myr after CAI formation^{7,8,29}. However, deriving initial $^{53}\text{Mn}/^{55}\text{Mn}$ ratios of carbonate based on in-situ SIMS analyses requires standards that closely match the chemical composition of the target mineral to constrain the Mn/Cr ratio accurately (e.g., are 'matrix-matched'), particularly with regard to the Fe content of the carbonate³⁰⁻³². Previous studies which targeted dolomite were performed using non-matrix-matched standards (primarily calcite) for the Mn/Cr ratio, which can affect the accuracy of the results^{31,32}. In this work, we use matrix-matched calcite, dolomite, and magnesite standards obtain the Mn/Cr ratios of respective mineral phases in Ryugu.

Ryugu particles A0037 and C0009, which were acquired from the 1st and 2nd touchdown sites respectively³, are dominated by minerals produced via aqueous alteration^{1,3}. A0037 contains a much higher abundance of carbonate (21.2 vol%) than C0009 (1.8 vol%)³. Carbonates found in these two particles are primarily dolomite ($\text{CaMg}(\text{CO}_3)_2$, Fig. 1a; see also Fig. 2 in Yamaguchi et al., 2022) with minor occurrence of Ca-carbonate (CaCO_3 , Fig. 1b; see also Supplementary Fig. 6 in Yamaguchi et al., 2022) and breunnerite ($(\text{Mg,Fe,Mn})\text{CO}_3$, see Supplementary Fig. 6 in Yamaguchi et al., 2022) in C0009. Both particles contain magnetite (3.6 vol%)³ with a variety of morphologies, often enclosed within dolomite (Fig. 1a, see also Supplementary Fig. 6 in Yamaguchi et al., 2022). Detailed petrological and mineralogical descriptions of both particles are given by Ito et al. 2022 and Yamaguchi et al. 2022.

Results

Oxygen isotopic composition of carbonate and magnetite

The oxygen isotopic compositions of dolomite in particles A0037 and C0009, magnetite in particle A0037, and Ca-carbonate in C0009 are shown in Fig. 2 and are summarized in Supplementary Tables 1–3. The oxygen isotopic compositions of dolomites mostly plot near the terrestrial mass fractionation (TF) line; however several dolomite grains have positive $\Delta^{17}\text{O}$ well resolved from 0‰, ranging up to a maximum of $+1.6 \pm 0.3\text{‰}$ (2s) for an A0037 dolomite grain. The $\delta^{18}\text{O}$ values of dolomite grains are also somewhat variable, ranging from $+25\text{‰}$ to $+34\text{‰}$. The range of oxygen isotopic compositions of Ryugu dolomite is in good agreement with prior in-situ analyses of CI-chondrite dolomite²⁰ (see Fig. 2). The $\Delta^{17}\text{O}$ values of magnetite in A0037 show a limited range from $+2.1\text{‰}$ to $+3.9\text{‰}$ which nevertheless exceeds analytical uncertainty (MSWD = 5.2). The variation of $\delta^{18}\text{O}$ values among 4 grains measured are likewise small, ranging from $+1\text{‰}$ to $+3\text{‰}$. These $\delta^{18}\text{O}$ and $\Delta^{17}\text{O}$ values are similar to those observed in bulk analyses of CI chondrite magnetite¹⁰ (see Fig. 2). In contrast, the Ca-carbonate found in particle C0009 ranges in composition from $\Delta^{17}\text{O} \sim 0$ to $+2.2\text{‰}$ and $\delta^{18}\text{O} \sim +34\text{‰}$ to $+39\text{‰}$, which differs significantly from $\Delta^{17}\text{O} \sim 0\text{‰}$ and $\delta^{18}\text{O} = +25.5\text{‰}$ found in calcite separated from Orgueil²⁰.

Carbon isotopic compositions of carbonate

Dolomite in both Ryugu particles show a range of $\delta^{13}\text{C}$ values from 55.4‰ to 74.5‰ (Fig. 3 and Supplementary Table 4). Dolomite in A0037 appears to follow a bimodal distribution with $\delta^{13}\text{C}$ peaks at ~ 55 and $\sim 70\text{‰}$. Dolomite (and some Ca-carbonate) in C0009 show a range of 64‰ to 75‰ , with one Ca-carbonate enriched in $\delta^{13}\text{C}$ at 97‰ (Fig. 3 and Supplementary Table 4). These $\delta^{13}\text{C}$ values are consistent with bulk measurements of Orgueil carbonates²⁴.

Mn-Cr dating of carbonate

We measured $^{55}\text{Mn}/^{52}\text{Cr}$ and $^{53}\text{Cr}/^{52}\text{Cr}$ ratios for 20 spots on dolomite in A0037 and 16 spots on dolomite, breunnerite, and calcite in C0009 and corrected for the relative sensitivity between Mn and Cr

using matrix-matched, ^{52}Cr -implanted terrestrial carbonate standards. The analysis conditions, standards development, and Mn-Cr data on Ryugu carbonates are detailed in the Supplementary Information. The data show ^{53}Cr excesses that are well-correlated with $^{55}\text{Mn}/^{52}\text{Cr}$ (Fig. 4) implying initial $^{53}\text{Mn}/^{55}\text{Mn}$ of $6.8 \pm 0.5 \times 10^{-6}$ (MSWD = 0.7) for A0037 dolomite and $6.1 \pm 0.9 \times 10^{-6}$ (MSWD = 0.3) for C0009 (all errors 2SE). By calibrating these initial ratios relative to the initial $^{53}\text{Mn}/^{55}\text{Mn}$ ratio³³ of the D'Orbigny angrite, which has a well-defined absolute crystallization age^{34,35}, we calculate that A0037 and C0009 carbonates formed at 4566.9 ± 0.4 Ma and 4566.3 ± 0.8 Ma, respectively. Assuming 'time-zero' defined by a $^{207}\text{Pb}/^{206}\text{Pb}$ closure age³⁶ for CAIs of 4567.3 Ma, the carbonates in Ryugu formed within the first 1.4 Myr of solar system origin—earlier than inferred from previous studies^{7,8,29}.

Discussion

A Ca-carbonate grain designated 'Ca 2' has $\Delta^{17}\text{O} = +2.2\text{‰}$, the highest value of $\Delta^{17}\text{O}$ we have measured in Ryugu carbonate, which suggests that it recorded an early phase of fluid evolution when relatively ^{17}O - and ^{18}O -enriched fluid²¹ was less equilibrated with ^{16}O -rich nebular solids²². The petrology of 'Ca 2' is distinct from the other Ca-carbonates, further supporting that its formation conditions were distinct from the other Ca-carbonates³⁷. Figure 3 shows that 'Ca 2' is also enriched in ^{13}C at $\delta^{13}\text{C} = +96.9\text{‰}$, suggesting that carbon in the fluid was initially isotopically heavy and derived from outer solar system CO_2 ices, similar to what has been inferred for some carbonaceous chondrites^{25,26,38}. Therefore, we conclude that Ryugu accreted in the outer solar system beyond the CO_2 ice line, consistent with previous observations of bulk H and N isotopes that are consistent with an outer solar system origin³.

The population of Ca-carbonate in particle C0009 shows a range in $\Delta^{17}\text{O}$ of ~ 0 to $+2.2\text{‰}$, following a mass-independent trend which requires that the O isotopic composition of the fluid evolved over the course of Ca-carbonate precipitation. This is in contrast to calcite grains found in Orgueil²⁰, which follow a mass-dependent trend with constant $\Delta^{17}\text{O}$ with a restricted range in $\delta^{18}\text{O}$. We suggest that this difference reflects variation in alteration processes between Ryugu and Orgueil: The Ca-carbonate in Ryugu recorded the progress of equilibration between fluid and ^{16}O -poor anhydrous silicate²², while calcite in Orgueil precipitated after this equilibration had occurred.

Magnetite in A0037 and the "Ca 2" Ca-carbonate grain (Fig. 1b; see also Fig. 4b in Yamaguchi et al., 2022) in C0009 share the same $\Delta^{17}\text{O}$ values (within uncertainty) that is higher than the $\Delta^{17}\text{O}$ of dolomite and other Ca-carbonates, reflecting a less-equilibrated fluid composition. We conclude that magnetite and Ca-carbonate like 'Ca 2' were among the earliest minerals to precipitate during the alteration of the Ryugu protolith, predating most carbonate formation. Though magnetite in A0037 and 'Ca 2' in C0009 are from different particles, if we assume that alteration was sufficiently widespread on the Ryugu parent body so that 'Ca 2' and A0037 magnetite formed in equilibrium³⁷, we estimate the formation temperature at this early stage of alteration using equilibrium thermometry of calcite and magnetite to be $0 - 20^\circ\text{C}$ ³⁹. Further

discussion of magnetite-H₂O and calcite-H₂O fractionation can be found in the Supplementary Information.

Dolomite in this study and bulk Ryugu particles share a value of $\Delta^{17}\text{O}$ within our uncertainties⁴. The bulk oxygen isotopic composition is dominated by phyllosilicates, with variable contributions from carbonates which can increase the $\delta^{18}\text{O}$ of the bulk analysis. If we suppose that the weighted average of bulk Ryugu $\delta^{18}\text{O}$ from Greenwood et al., 2022 of $15.88 \pm 4.85\text{‰}$ (2SD) represents the composition of phyllosilicate, we may calculate an equilibrium formation temperature using this phyllosilicate-dominated bulk analysis and our observed range of dolomite $\delta^{18}\text{O}$ values (+ 25–34‰). Using experimentally-determined fractionation factors for dolomite⁴⁰ and brucite⁴¹, we constrain the equilibration temperature of dolomite and phyllosilicate to 88–240°C. Further discussion of phyllosilicate-H₂O and dolomite-H₂O fractionation can be found in the Supplementary Information.

We suggest the following order for the sequence of aqueous alteration on Ryugu: first, magnetite and Ca-carbonates like 'Ca 2' precipitated from aqueous fluids with high $\Delta^{17}\text{O}$ at $T < 20^\circ\text{C}$ with C composition dominated by CO₂ ice. As the fluid continued to exchange oxygen with ¹⁶O-rich anhydrous silicates²², additional Ca-carbonate precipitated as $\Delta^{17}\text{O}$ fell from $\sim + 1.1$ to 0‰. Finally, most dolomite formed at about $\Delta^{17}\text{O} = + 0.4\text{‰}$ after Mg had been added to the fluid by alteration of Mg-rich silicates to form phyllosilicates with similar $\Delta^{17}\text{O}$ to dolomite. The relatively homogeneous $\Delta^{17}\text{O}$ composition of dolomite indicates that the pace of evolution of the fluid's oxygen isotopic composition had slowed by the time of dolomite formation. Petrographic observations of magnetite inclusions enclosed in dolomite but not in calcite support this sequence of events³⁷.

Carbon and oxygen isotopic analyses performed on the same grains were used to explore correlations between the two isotopic systems. Figure 5 illustrates that $\delta^{13}\text{C}$ is correlated with $\delta^{18}\text{O}$ (upper panel) and $\Delta^{17}\text{O}$ (lower panel), similar to trends observed for some CM chondrites²⁸. This observation suggests that methane formation via serpentinization of the protolith followed by loss to space did not strongly affect the $\delta^{13}\text{C}$ of Ryugu carbonate, as methane release would enrich ¹³C in the fluid over time^{16,27}. In contrast, we observe that carbonate formed from less-equilibrated water (e.g., with higher $\delta^{18}\text{O}$ and $\Delta^{17}\text{O}$) is also the most enriched in $\delta^{13}\text{C}$. One possible scenario could be that the initial unequilibrated fluid composition, presumably similar to the fluid recorded by 'Ca 2', evolved towards lower $\delta^{13}\text{C}$ as the fluid interacted with and oxidized Ryugu's relatively ¹³C-depleted organic matter³.

The old ages measured in Ryugu carbonate stand in contrast to ages obtained from carbonate in carbonaceous chondrites, most of which were thought to have formed 4–6 Myr after CAIs^{7,8,29}. This difference arises from our use of matrix-matched standards, as opposed to calcite standards used exclusively in previous studies, to determine the Mn/Cr of the carbonates. Had we corrected measured Mn⁺/Cr⁺ using a relative sensitivity factor derived only from analyses of calcite, we would have obtained

ages of 3.0 Myr and 3.5 Myr after CAI formation for A0037 and C0009 carbonate respectively, approaching the range of ages previously determined for carbonates in carbonaceous chondrites^{7,8,29}.

These old carbonate formation ages suggest a significantly different formation scenario for Ryugu than those previously proposed for the asteroid parent bodies of carbonaceous chondrites. Our data clearly show that aqueous fluids responsible for carbonate formation were active on Ryugu (or its progenitor asteroid) early in Solar System history, within the first ~ 1.4 Myr after CAI formation. At that time, ^{26}Al in chondritic material was still at the level of $^{26}\text{Al}/^{27}\text{Al} \sim 10^{-5}$, abundant enough to melt accreted ices and drive aqueous alteration. However, for ^{26}Al heating to not be so intensive as to cause water loss or even silicate melting and chemical differentiation, Ryugu must have accreted as a small asteroid which could effectively conduct heat away from its interior to cool itself by radiation. The inferred presence of co-accreted CO_2 ice constrains the initial temperature of the parent body to below the sublimation temperature of CO_2 . By modeling parent bodies accreting as mixtures of 50% chondritic material and 50% water ice^{6,42} at an initial temperature of 78 K, we find that parent bodies accreting before 1.4 Myr must be smaller than 17 km in diameter for the internal temperature to remain below 400 K^{43,44}. In these bodies, the interior 4 km reaches the melting point of water within 0.2 Myr after accretion, and remains warm enough to support liquid water for an additional 1.5 Myr.

Alternatively, it could be possible to form Ryugu components in a progenitor body larger than 17 km in diameter which was later disrupted by impact before reaching peak temperatures. Ryugu is a ~ 1 km diameter asteroid inferred, like many asteroids, to be a 'rubble pile' characterized by large internal void spaces and a low bulk density ($1,190 \pm 20 \text{ kg m}^{-3}$)⁴⁵. A multi-stage scenario of brecciation and reassembly is also supported by petrographic and shock characteristics observed in Ryugu particles^{3,37,46}. This view is very different from prior estimates of parent body size and accretion times based upon younger carbonate ages, which suggested that CM and CI parent bodies were > 50 km in diameter and accreted $\sim 3\text{--}3.5$ Myr after CAI formation^{7,8,29}.

An early formation scenario for C-type asteroids has implications for models seeking to understand the origins of the so-called 'isotopic dichotomy' within the solar nebula. In this framework, the early solar system was divided into two reservoirs, one characterized by isotopic compositions similar to those of the volatile-rich carbonaceous chondrites (CC), and the other being isotopically similar to the compositions of volatile-depleted ordinary-chondrite, enstatite-chondrite, and terrestrial (collectively known as the non-carbonaceous (NC) isotopic reservoir) materials⁴⁷. Whereas the NC group accreted from materials formed in the inner solar system, the CC group is thought to have accreted in the outer solar system, beyond the snow line. Based on $^{182}\text{Hf}\text{--}^{182}\text{W}$ ages of iron meteorites with CC affinities, it has been suggested that some planetesimals in the outer solar system accreted within ~ 1 Myr of CAI formation⁴⁸. This timescale is consistent with such objects having melted and chemically differentiated into core-mantle structures due to ^{26}Al heating, and is also consistent with the accretion time of NWA 011, a basaltic achondrite with CC affinities that accreted within 1.6 Myr of CAI formation⁴⁹. Based on previous Mn-Cr dating of carbonates it was thought that CM and CI chondrites escaped such heating by

virtue of having accreted at later times, after most ^{26}Al had decayed. However, early formation for undifferentiated CC material, such as that from Ryugu, requires an explanation (e.g., formation in a small body or early disruption by impact) for the simultaneous existence of differentiated and unmelted CC materials. Similarly, models of accretion and transport in the disk which invoke a late formation time for carbonaceous chondrite parent bodies⁵⁰ should consider the implications of early formation of these objects.

References

1. Yada, T. *et al.* Preliminary analysis of the Hayabusa2 samples returned from C-type asteroid Ryugu. *Nature Astronomy* **6**, 214–220 (2022).
2. Pilorget, C. *et al.* First compositional analysis of Ryugu samples by the MicrOmega hyperspectral microscope. *Nature Astronomy* **6**, 221–225 (2022).
3. Ito, M., Tomioka, N., Uesugi, M., Yamaguchi, A. & Shirai, N.
4. Greenwood, R. C. *et al.* Oxygen isotope analysis of Ryugu particles: Fresh evidence for hydration of Earth by CI chondrites. *Nature Astronomy* (2022).
5. Leshin, L. A., Rubin, A. E. & McKeegan, K. D. The oxygen isotopic composition of olivine and pyroxene from CI chondrites. *Geochimica et Cosmochimica Acta* **61**, 835–845 (1997).
6. Clayton, R. N. & Mayeda, T. K. Oxygen isotope studies of carbonaceous chondrites. *Geochimica et Cosmochimica Acta* **63**, 2089–2104 (1999).
7. Fujiya, W., Sugiura, N., Sano, Y. & Hiyagon, H. Mn–Cr ages of dolomites in CI chondrites and the Tagish Lake ungrouped carbonaceous chondrite. *Earth and Planetary Science Letters* **362**, 130–142 (2013).
8. Visser, R., John, T., Whitehouse, M. J., Patzek, M. & Bischoff, A. A short-lived ^{26}Al induced hydrothermal alteration event in the outer solar system: Constraints from Mn/Cr ages of carbonates. *Earth and Planetary Science Letters* **547**, 116440 (2020).
9. Clayton, R. N. & Mayeda, T. K. The oxygen isotope record in Murchison and other carbonaceous chondrites. *Earth and Planetary Science Letters* **67**, 151–161 (1984).
10. Rowe, M. W., Clayton, R. N. & Mayeda, T. K. Oxygen isotopes in separated components of CI and CM meteorites. *Geochimica et Cosmochimica Acta* **58**, 5341–5347 (1994).
11. Tyra, M. A., Farquhar, J., Guan, Y. & Leshin, L. A. An oxygen isotope dichotomy in CM2 chondritic carbonates—A SIMS approach. *Geochimica et Cosmochimica Acta* **77**, 383–395 (2012).
12. Lee, M. R., Sofo, M. R., Lindgren, P., Starkey, N. A. & Franchi, I. A. The oxygen isotope evolution of parent body aqueous solutions as recorded by multiple carbonate generations in the Lonewolf Nunataks 94101 CM2 carbonaceous chondrite. *Geochimica et Cosmochimica Acta* **121**, 452–466 (2013).
13. Lee, M. R., Lindgren, P. & Sofo, M. R. Aragonite, breunnerite, calcite and dolomite in the CM carbonaceous chondrites: High fidelity recorders of progressive parent body aqueous alteration.

- Geochimica et Cosmochimica Acta **144**, 126–156 (2014).
14. Fujiya, W. *et al.* Comprehensive study of carbon and oxygen isotopic compositions, trace element abundances, and cathodoluminescence intensities of calcite in the Murchison CM chondrite. *Geochimica et Cosmochimica Acta* **161**, 101–117 (2015).
 15. Tyra, M., Brearley, A. & Guan, Y. Episodic carbonate precipitation in the CM chondrite ALH 84049: An ion microprobe analysis of O and C isotopes. *Geochimica et Cosmochimica Acta* **175**, 195–207 (2016).
 16. Vacher, L. G., Marrocchi, Y., Villeneuve, J., Verdier-Paoletti, M. J. & Gounelle, M. Petrographic and C & O isotopic characteristics of the earliest stages of aqueous alteration of CM chondrites. *Geochimica et Cosmochimica Acta* **213**, 271–290 (2017).
 17. Verdier-Paoletti, M. J. *et al.* Oxygen isotope constraints on the alteration temperatures of CM chondrites. *Earth and Planetary Science Letters* **458**, 273–281 (2017).
 18. Vacher, L. G., Marrocchi, Y., Villeneuve, J., Verdier-Paoletti, M. J. & Gounelle, M. Collisional and alteration history of the CM parent body. *Geochimica et Cosmochimica Acta* **239**, 213–234 (2018).
 19. Telus, M., Alexander, C. M. O., Hauri, E. H. & Wang, J. Calcite and dolomite formation in the CM parent body: Insight from in situ C and O isotope analyses. *Geochimica et Cosmochimica Acta* **260**, 275–291 (2019).
 20. Piralla, M. *et al.* Primordial water and dust of the Solar System: Insights from in situ oxygen measurements of CI chondrites. *Geochimica et Cosmochimica Acta* **269**, 451–464 (2020).
 21. Sakamoto, N. *et al.* Remnants of the Early Solar System Water Enriched in Heavy Oxygen Isotopes. *Science* (2007) doi:10.1126/science.1142021.
 22. Liu, M.-C. *et al.* Incorporation of ¹⁶O-rich anhydrous silicates in the protolith of highly hydrated asteroid Ryugu. *Nature Astronomy* (2022).
 23. Alexander, C. M. O., Fogel, M., Yabuta, H. & Cody, G. D. The origin and evolution of chondrites recorded in the elemental and isotopic compositions of their macromolecular organic matter. *Geochimica et Cosmochimica Acta* **71**, 4380–4403 (2007).
 24. Sephton, M. A., Pillinger, C. T. & Gilmour, I. Aromatic moieties in meteoritic macromolecular materials: analyses by hydrous pyrolysis and $\delta^{13}\text{C}$ of individual compounds. *Geochimica et Cosmochimica Acta* **64**, 321–328 (2000).
 25. Hässig, M. *et al.* Isotopic composition of CO₂ in the coma of 67P/Churyumov-Gerasimenko measured with ROSINA/DFMS. *A&A* **605**, A50 (2017).
 26. Fujiya, W., Aoki, Y., Ushikubo, T., Hashizume, K. & Yamaguchi, A. Carbon isotopic evolution of aqueous fluids in CM chondrites: Clues from in-situ isotope analyses within calcite grains in Yamato-791198. *Geochimica et Cosmochimica Acta* **274**, 246–260 (2020).
 27. Guo, W. & Eiler, J. M. Temperatures of aqueous alteration and evidence for methane generation on the parent bodies of the CM chondrites. *Geochimica et Cosmochimica Acta* **71**, 5565–5575 (2007).

28. Alexander, C. M. O., Bowden, R., Fogel, M. L. & Howard, K. T. Carbonate abundances and isotopic compositions in chondrites. *Meteorit Planet Sci* **50**, 810–833 (2015).
29. Fujiya, W., Sugiura, N., Hotta, H., Ichimura, K. & Sano, Y. Evidence for the late formation of hydrous asteroids from young meteoritic carbonates. *Nat Commun* **3**, 627 (2012).
30. Sugiura, N. & Ichimura, K. Mn/Cr relative sensitivity factors for synthetic calcium carbonate measured with a NanoSIMS ion microprobe. *Geochemical Journal* **44**, e11-316 (2010).
31. Steele, R. C. J., Heber, V. S. & McKeegan, K. D. Matrix effects on the relative sensitivity factors for manganese and chromium during ion microprobe analysis of carbonate: Implications for early Solar System chronology. *Geochimica et Cosmochimica Acta* **201**, 245–259 (2017).
32. McCain, K. A., Liu, M.-C. & McKeegan, K. D. Calibration of matrix-dependent biases in isotope and trace element analyses of carbonate minerals. *Journal of Vacuum Science & Technology B* **38**, 044005 (2020).
33. McKibbin, S. J., Ireland, T. R., Amelin, Y. & Holden, P. Mn–Cr dating of Fe- and Ca-rich olivine from ‘quenched’ and ‘plutonic’ angrite meteorites using Secondary Ion Mass Spectrometry. *Geochimica et Cosmochimica Acta* **157**, 13–27 (2015).
34. Brennecka, G. A. & Wadhwa, M. Uranium isotope compositions of the basaltic angrite meteorites and the chronological implications for the early Solar System. *PNAS* **109**, 9299–9303 (2012).
35. Amelin, Y. U–Pb ages of angrites. *Geochimica et Cosmochimica Acta* **72**, 221–232 (2008).
36. Amelin, Y. *et al.* U–Pb chronology of the Solar System’s oldest solids with variable $^{238}\text{U}/^{235}\text{U}$. *Earth and Planetary Science Letters* **300**, 343–350 (2010).
37. Yamaguchi, A. *et al.* Complex geologic history of C-type asteroids: Fresh insights from the analysis of Ryugu particles. *Nature Astronomy* (2022).
38. Fujiya, W. *et al.* Migration of D-type asteroids from the outer Solar System inferred from carbonate in meteorites. *Nature Astronomy* **1** (2019) doi:10.1038/s41550-019-0801-4.
39. Hayles, J., Gao, C., Cao, X., Liu, Y. & Bao, H. Theoretical calibration of the triple oxygen isotope thermometer. *Geochimica et Cosmochimica Acta* **235**, 237–245 (2018).
40. Horita, J. Oxygen and carbon isotope fractionation in the system dolomite–water–CO₂ to elevated temperatures. *Geochimica et Cosmochimica Acta* **129**, 111–124 (2014).
41. Saccocia, P. J., Seewald, J. S. & Shanks, W. C. Oxygen isotope fractionation in the portlandite–water and brucite–water systems from 125 to 450°C, 50MPa. *Geochimica et Cosmochimica Acta* **169**, 137–151 (2015).
42. Zolensky, M., Barrett, R. & Browning, L. Mineralogy and composition of matrix and chondrule rims in carbonaceous chondrites. *Geochimica et Cosmochimica Acta* **57**, 3123–3148 (1993).
43. McCain, K. A., Young, E. D. & Manning, C. E. CM Carbonates Should Be Old: Insights from Parent Body Thermal Modeling. in vol. 48 2181 (2017).
44. Zhou, Q. *et al.* SIMS Pb–Pb and U–Pb age determination of eucrite zircons at < 5 μm scale and the first 50 Ma of the thermal history of Vesta. *Geochimica et Cosmochimica Acta* **110**, 152–175 (2013).

45. Watanabe, S. *et al.* Hayabusa2 arrives at the carbonaceous asteroid 162173 Ryugu—A spinning top-shaped rubble pile. *Science* (2019) doi:10.1126/science.aav8032.
46. Tomioka, N. *et al.* Calibrating the shock regime experienced by the regolith particles of hydrated asteroid Ryugu. *Nature Astronomy* (2022).
47. Kleine, T. *et al.* The Non-carbonaceous–Carbonaceous Meteorite Dichotomy. *Space Sci Rev* **216**, 55 (2020).
48. Kruijer, T. S., Burkhardt, C., Budde, G. & Kleine, T. Age of Jupiter inferred from the distinct genetics and formation times of meteorites. *Proceedings of the National Academy of Sciences* **114**, 6712–6716 (2017).
49. Sugiura, N. & Fujiya, W. Correlated accretion ages and $\epsilon^{54}\text{Cr}$ of meteorite parent bodies and the evolution of the solar nebula. *Meteoritics & Planetary Science* **49**, 772–787 (2014).
50. Desch, S. J., Kalyaan, A. & Alexander, C. M. O. The Effect of Jupiter's Formation on the Distribution of Refractory Elements and Inclusions in Meteorites. *ApJS* **238**, 11 (2018).

Declarations

Data availability

Correspondence and requests for materials should be addressed to K.A.M and N.M. All analytical data related to this manuscript will be put on the JAXA Data ARchives and Transmission System (DARTS) after a one-year proprietary period.

Acknowledgements

We thank all scientists and engineers of the Hayabusa2 project whose dedication and skill brought these precious particles back to Earth. This research was supported in part by the JSPS KAKENHI (JP18K18795 and JP18H04468 to M.I., NESSF19R 19-PLANET19R-0001 to K.A.M., JP20H01965 to N.T., JP18H05479 [Innovative Areas “MFS Materials Science”] to M.U., JP19H01959 to A.Y., JP18K03729 to M.K., JP21K03652 to N.I., JP17H06459 to T.U., JP19K03958 to M.A., JP17H06459 to T.O., JP18K03830 to T.Y., JP19K23473, JP20K14548 to T.H., JP19K23474, JP21K13986 to D.Y., JP20K14535 to R.F., JP17H06459 and JP19H01951 to S.W.), and by the NIPR Research Project (KP307 to A.Y.). We thank Edward Young for discussions of the implications of the data and for the parent body modeling code. The UCLA ion microprobe facility is partially supported by a grant from the NSF Instrumentation and Facilities program. Ion implantation of carbonate standards was performed by CuttingEdge Ions.

Author contributions

K.A.M. and N.M led the project and wrote the initial draft. K.A.M., N.M., M-C.L., A.Y., N.T., M.I., M.U., N.I., N.S., T. Ohigashi, M.K., K.U., A.N., KY., H.Y., and Y.K. conducted sample handling, preparation, and mounting processes of Ryugu grains. M.I., N.T., T. Ohigashi, M.U., K.U., H.Y., Y.K., K.H., I.S., I.O., and K.U. developed universal sample holders for multiple instruments. A.Y., M.K., N.I., M.I., and N.T. performed SEM-EDS analysis. A.Y. conducted EPMA analysis and data reduction. K.A.M., N.M., and M.-C.L. carried out oxygen, carbon, and Mn-Cr isotopes measurements of anhydrous carbonate and magnetite with SIMS. A.N., K.Y., A.M., M.N., T.Y., T. Okada., M.A., and T.U lead the JAXA curation activities for initial characterization of allocated Ryugu particles. S.N., T. Okada., T.S., S.T., F.T., M.Y., S.W., and Y.T. administered the project and acted as principal investigators. All authors contributed to the data interpretation, commented on the earlier versions of the manuscript, and approved the final version of the manuscript for submission.

Competing interests

The authors declare no competing interests.

Additional information

Supplementary information is available for this paper: Supplementary online text, Supplementary Figures 1–4, and Supplementary Tables 1–7.

Figures

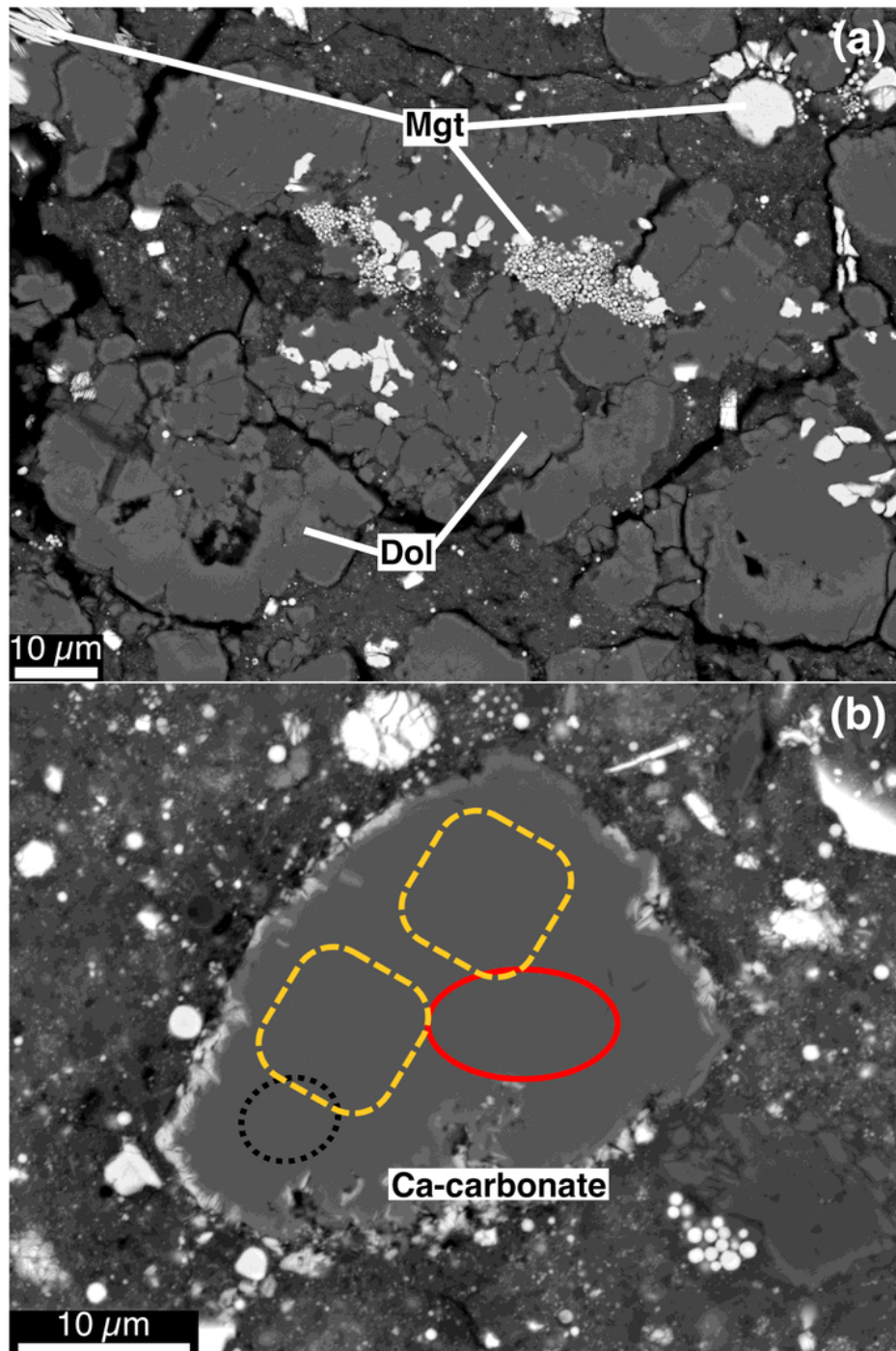


Figure 1

Backscattered electron (BSE) images of Ryugu particles (a) A0037 and (b) C0009³⁷. Dol: dolomite, Mgt: magnetite. The dotted black oval, red oval, and dashed yellow squares in (b) represent the size and location of the oxygen, carbon, and Mn-Cr analysis pits, respectively.

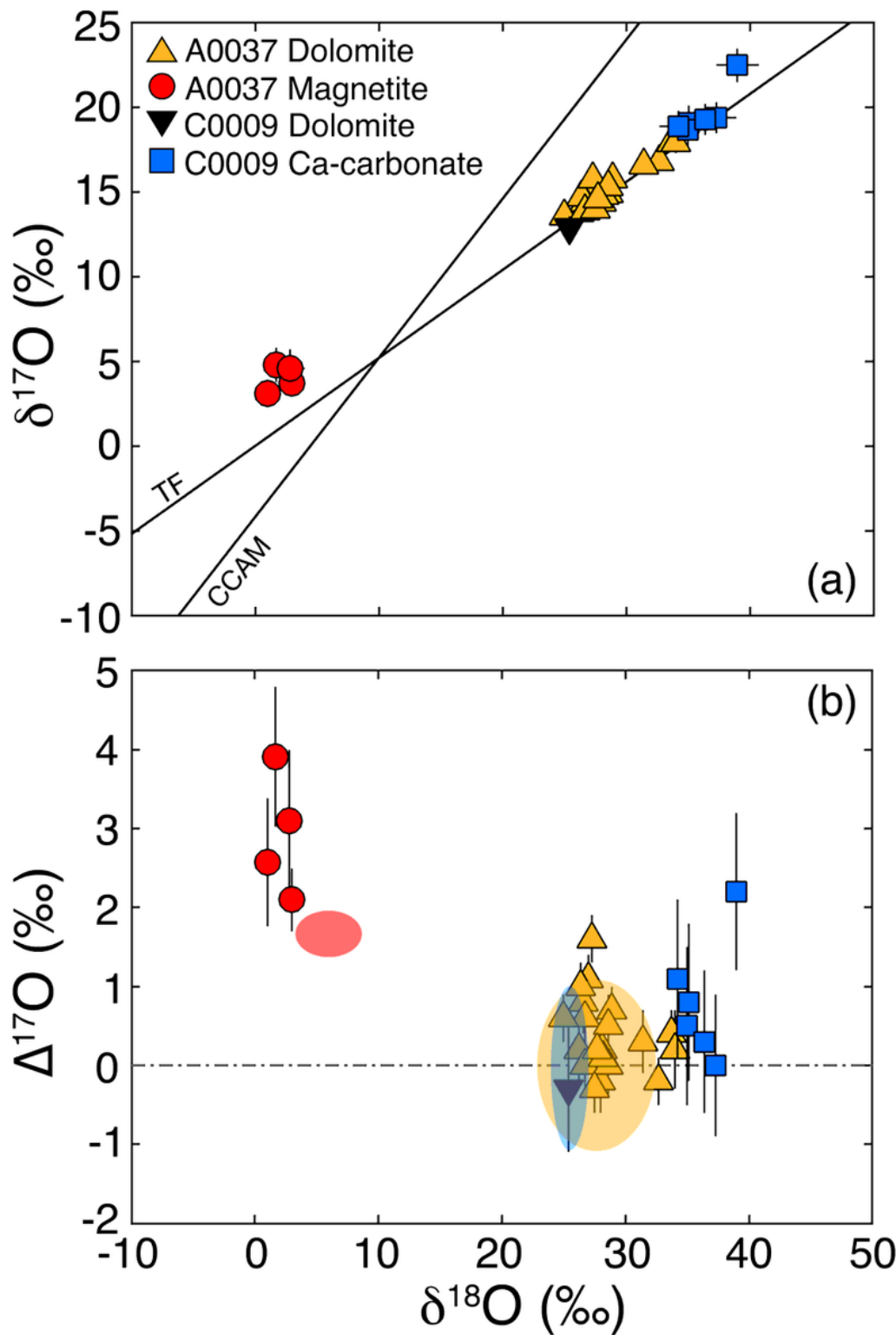


Figure 2

(a) A three-oxygen isotope diagram of carbonate and magnetite in Ryugu particles A00037 and C0009 relative to SMOW. The blue, yellow, and red shaded regions represent previous studies of in situ calcite, in situ dolomite, and bulk magnetite, respectively^{10,20}. Errors are 2σ standard errors. TF: terrestrial fractionation line, CCAM: carbonaceous chondrite anhydrous minerals line. (b) $\Delta^{17}\text{O}$ vs. $\delta^{18}\text{O}$ values of Ryugu carbonate and magnetite.

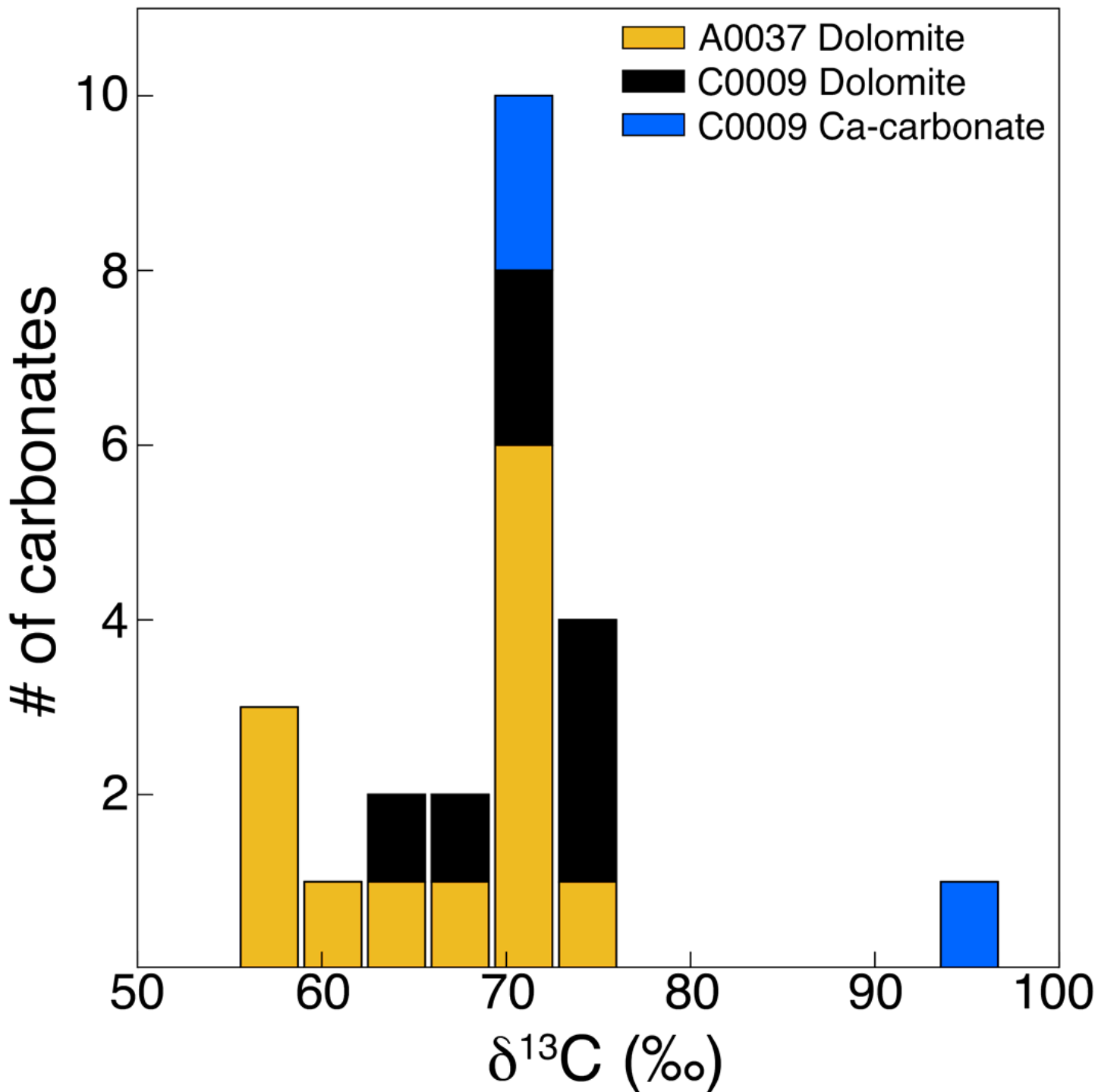


Figure 3

Stacked histogram of C isotopic compositions of carbonate in Ryugu particles A0037 and C0009 relative to VPDB. The Ca-carbonate outlier at $\delta^{13}\text{C} = 96 \text{ ‰}$ is 'Ca2' (see text).

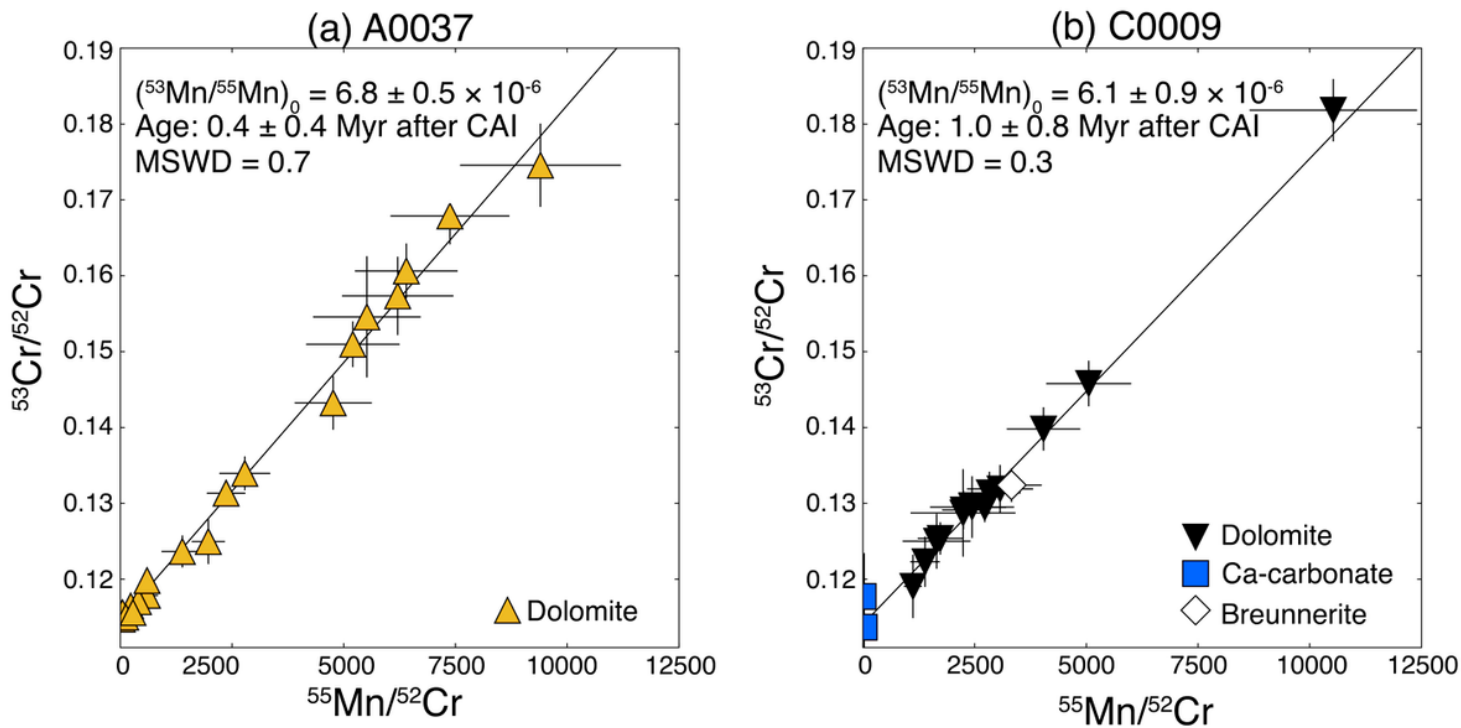


Figure 4

Mn-Cr isochrons for carbonates in Ryugu particles (a) A0037 and (b) C0009. Ages in Myr are reported relative to an absolute CAI age of 4567.3 Ma^{35} and anchored to the D'Orbigny angrite and $(^{53}\text{Mn}/^{55}\text{Mn})_0$ (see text). Error bars ($\pm 2\sigma$) represent external and internal error summed in quadrature.

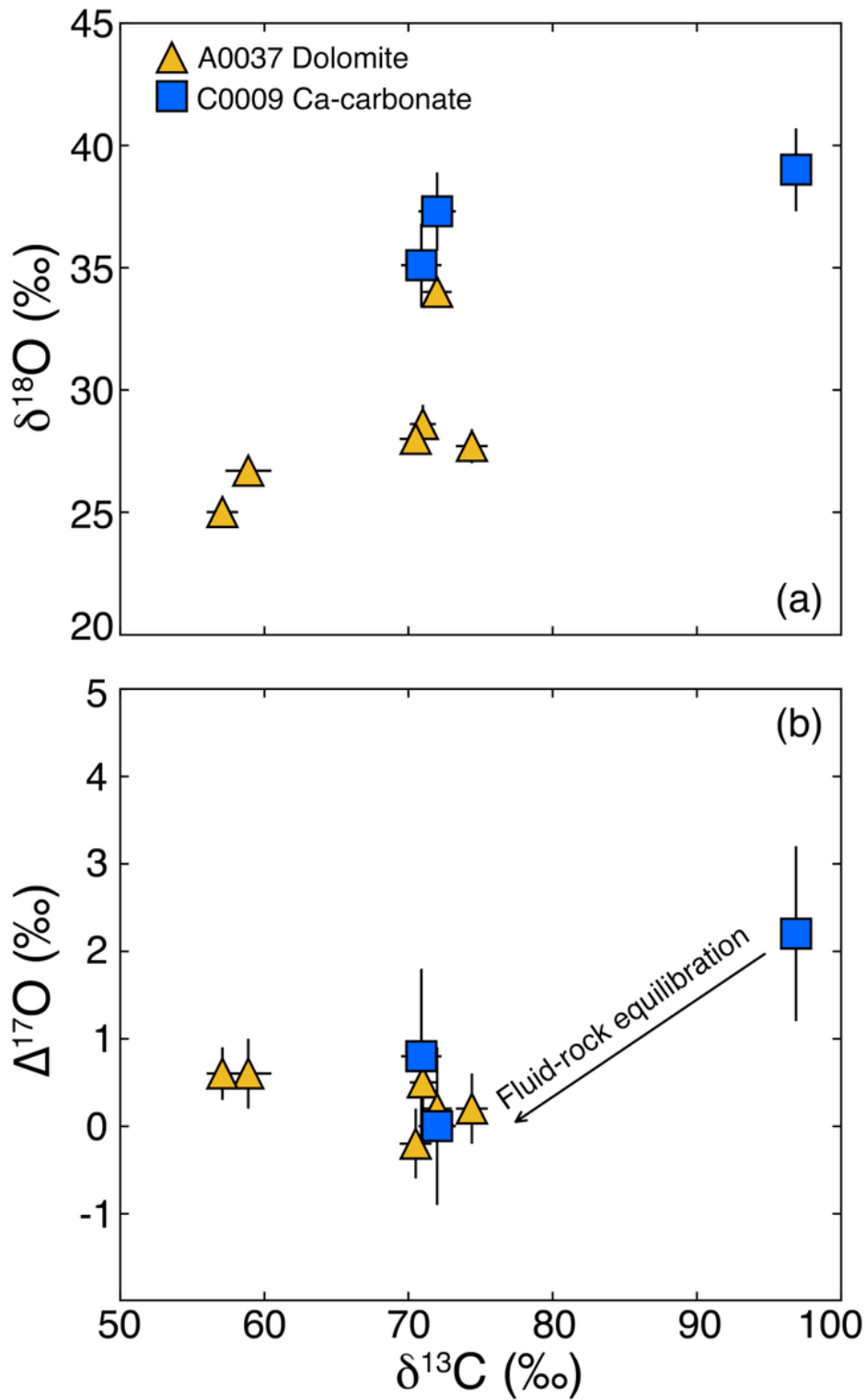


Figure 5

Carbon isotopic composition (relative to VPDB) of Ryugu dolomite (yellow triangles) and Ca-carbonate (blue squares) versus (a) $\delta^{18}\text{O}$ and (b) $\Delta^{17}\text{O}$ from the same carbonate grains.

Supplementary Files

This is a list of supplementary files associated with this preprint. Click to download.

- [McCainMatsudaSupplementary.docx](#)